Food Chemistry 496 (2025) 146781

Contents lists available at ScienceDirect

Food Chemistry

journal homepage: www.elsevier.com/locate/foodchem

Emulsion stabilization by sustainable yeast proteins from *Saccharomyces cerevisiae*: Influence of pH value and oil content☆

Laura Riedel *, Ulrike S. van der Schaaf

Karlsruhe Institute of Technology, Kaiserstr. 12, Karlsruhe, 76131, Germany

ARTICLE INFO

Keywords:
Single cell protein
Sustainable food
Biosurfactant
Food functionality
Emulsifying properties
Interfacial adsorption
Protein structure

ABSTRACT

This study investigates the potential application of alternative proteins from baker's yeast in food emulsions, examining how oil content and pH affect emulsion microstructure and stability. Emulsions were prepared at pH values of 3, 5, and 7, with oil contents up to 50 wt%. Measurement techniques like zeta potential, SDS-PAGE, light scattering, microscopy, and rheometry were used for characterization. At pH 5, partitioning occurred immediately after preparation, while at pH 3 and 7, emulsions appeared homogeneous. Droplet size and microscopic analysis showed different microstructures of the emulsions: individual droplets at pH 7, dense flocs at pH 5, and loosely packed flocs at pH 3. pH-induced aggregation and unfolding of the protein molecules due to acid treatment were key factors influencing the oil droplet structuring and therefore the emulsion stability. The study shows that yeast proteins can stabilize high oil-content emulsions and they offer a pathway for developing novel, eco-friendly emulsifiers for the food industry.

1. Introduction

With the continuous growth in the global population, the demand for adequate food supplies and nutrients such as proteins and vitamins is rising, too. Traditional protein sources such as meat and plant-based proteins are increasingly facing ecological and economic limitations (Gouel, 2017). In this context, yeast cells are emerging as a promising alternative protein source. Yeast cells are high in protein (40–60 wt% in dry matter) (Haehn, 1952; Narsipur, Kew, Ferreira, El-Gendy, & Sarkar, 2024; Schachtel, 1981; Yamada & Sgarbieri, 2005). They can be produced sustainably as yeasts can metabolize side streams, e.g. from the food industry, and have a high reproduction rate. Additionally, their cultivation bears the advantages of decentralized production and of being independent of weather conditions. Moreover, consumers already accept them because they have been used in foods for a long time (Jach, Serefko, Ziaja, & Kieliszek, 2022; Kinsella & Shetty, 1978; Nasseri, Rasoul-Amini, Morowvat, & Ghasemi, 2011; Spalvins, Zihare, & Blumberga, 2018; Tonnius, 1982).

To replace conventional proteins in foods with alternatives such as yeast proteins, it is essential to consider the nutritional composition and understand consumers' needs: Typically, fermented biomass such as from yeast cultivation is not consumed directly. Instead, the obtained proteins will be formulated into attractive food products. Yeast proteins offer the possibility to replace dairy or plant proteins in emulsion-based products such as yogurts, spreads, sauces, desserts, and the like. For this purpose, it is necessary to understand their functional properties in terms of emulsion stabilization. With this knowledge, processes and product formulations can be adapted to different requirements of alternative protein sources.

Yeast cells can be involved in the stabilization of oil–water-interfaces in various ways, e.g. as whole cells in the form of pickering particles, through large protein-based particles or through significantly smaller, individual protein molecules that attach to the oil–water interface (Cheng et al., 2024; Firoozmand & Rousseau, 2016; Moreira, da Silva, Gombert, & da Cunha, 2016; Narsipur et al., 2024). There are two main types of proteins in yeast cells that can be distinguished: Mannoproteins attached to the outer side of the cell wall and various intracellular proteins. The emulsion stabilizing properties of outer cell wall mannoproteins have already been described (Barriga, Cooper, Idziak, & Cameron, 1999; Cameron, Cooper, & Neufeld, 1988; Heeres, Picone, van der Wielen, Cunha, & Cuellar, 2014; Li, Karboune, & Asehraou, 2020; Qiao et al., 2022). In contrast, much less is known about the emulsion-stabilizing properties of the intracellular proteins, used in the present study. These proteins are obtained after cell disruption (Hedenskog & Mogren, 1973; Kampen, 2005; Lee, Kim, Jo, & Choi, 2024; Ma, Sun, Meng, Zhou, Zhang, & Yang, 2023; Otero, Wagner, Vasallo, Garcıa, & Añón, 2000; Overbeck, Michel, Kampen,

☆ This article is part of a Special issue entitled: '3rd NIZO Plant Protein' published in Food Chemistry.

* Corresponding author.
E-mail addresses: laura.riedel@kit.edu (L. Riedel), ulrike.schaaf@kit.edu (U.S. van der Schaaf).

https://doi.org/10.1016/j.foodchem.2025.146781
Received 8 January 2025; Received in revised form 14 October 2025; Accepted 17 October 2025
Available online 30 October 2025

& Kwade, 2023; Pittroff, 1993; Sceni, Palazolo, Del Vasallo, Puppo, Otero, & Wagner, 2009). Since mannoproteins are bound to the cell wall, it is assumed that the protein solution used is free of these, as the cell suspension is centrifuged after breaking up and the precipitate, consisting of the cell wall material and thus the mannoproteins bound to it, is discarded.

It is known that proteins in general have surface-active properties due to their molecular structure (Damodaran, 2005; Kim, Wang, & Selomulya, 2020). The stabilization of emulsion droplets by proteins is a more complex process than, for example, the attachment of small synthetic emulsifier molecules to an oil–water interface and requires the amphiphilic molecules to migrate, adsorb, and unfold at the interface (Damodaran, 2005). The extent of the unfolding depends among other things on the type of protein and the timing (early adsorption or later one) (Bergfreund, Bertsch, & Fischer, 2021). Yeast proteins obtained by cell disruption also exhibit surface-active properties: For example, Lee et al. (2024) found that yeast protein isolate (YPI) has a similar emulsification activity to soy or pea protein isolate, but a lower one compared to whey protein isolate. Yeast proteins have a high proportion of hydrophobic amino acids. Ma, Xia, et al. (2023) introduced the H_0 value as a measure of a protein's hydrophobicity. To determine the surface hydrophobicity of the proteins, ANS (8-anilino-1-naphthalene sulfonic acid) is used for fluorescence labeling. The H_0 value is calculated from the initial slope of the fluorescence intensity, which is plotted against the protein concentration. A higher H_0 value indicates more hydrophobic amino acids. Yeast proteins, with a H_0 value of 520.5 ± 2.56, are highly hydrophobic, similar to pea protein (566.52 ± 10.04), while, for example, soy protein has a significantly lower H_0 value (220.04 ± 2.86). The high hydrophobicity compared to other proteins allows the yeast proteins to adsorb better to oil droplets but makes them more water-insoluble (Ma, Xia, et al., 2023). Pearce and Kinsella (1978) also investigated the emulsion stabilizing properties of YPI and found that they are comparatively poor, but can be significantly improved by functionalization of the protein, for example by succinylation.

In addition to adsorption, unfolding of the proteins at the interface is also important to protect the oil droplets against, for example, coalescence. According to Damodaran (2005), the structure of the protein is crucial in determining how quickly it can unfold or reorient at the interface. Highly structured proteins, such as bovine serum albumin, have poorer interfacial activity and unfold more slowly (Damodaran, 2005). It is possible that intracellular yeast proteins also tend to unfold slowly because as soluble proteins they will mainly be globular. Vananuvat and Kinsella (1975) investigated how the extraction method influences the functional properties of yeast proteins, but examined yeast cells from a different species (*Saccharomyces fragilis*). They found that the extraction method has a major influence on the emulsion stabilizing properties and that aqueous extraction followed by precipitation at pH 4 gave the best results of the methods considered.

In addition to the extraction method, the emulsion formulation, e.g. pH value and oil content, will influence how efficiently and effectively yeast protein can stabilize oil-in-water emulsions. Therefore, this study aims to understand how proteins from the interior of yeast cells behave under these conditions at the interface to use them as a protein source or as a functional ingredient in emulsion-based foods in the future. To the best of our knowledge, this has not yet been described.

To make the proteins usable as economically as possible and alter them as little as possible, fresh yeast was treated for cell disruption in a high-pressure homogenizer, and only solid cell components were removed by centrifugation without further extraction or purification of the proteins. This allowed us to investigate the functional properties of the proteins that were previously dissolved inside the cell separately from other cell components, such as the mannoproteins from the cell wall.

To investigate the behavior of the proteins at the interface under different pH values, it was essential to consider other protein properties under these conditions, such as charge, size, and aggregation, as they, in turn, can affect interfacial activity. After a comprehensive examination of the supernatant with all soluble cell components, it was used to produce emulsions with varying pH values, but also at different oil contents. The aim was to investigate whether emulsions with higher contents of dispersed phase could also be stabilized by yeast proteins to enable application for various products in the future, even with higher oil contents.

Both the macroscopic impression as well as microscopic images and the measurement of the droplet size distribution were used to evaluate the behavior of the proteins and their stabilization properties under changing formulation conditions.

2. Material and methods

Unless otherwise stated, demineralized water was used.

2.1. Yeast (*Saccharomyces cerevisiae*)

Yeast was purchased as cubed fresh yeast from a local supermarket. The cubes were stored at −23 °C until use. The required yeast cubes were thawed overnight in the refrigerator at 6 °C for further use.

2.2. Cell disruption and separation of the supernatant

For cell disruption, a suspension of 20 wt% yeast cube solution was prepared, cooled to 13 °C in an ice bath and disrupted in a high-pressure homogenizer at 1200 bar in one pass (Microfluidizer M-110EH with a y-reaction chamber, Microfluidics Cooperation, Newton, MA, USA). Immediately after the high-pressure homogenizer, the suspension was cooled to room temperature and centrifuged at 4250 rpm in an Eppendorf 5920 R centrifuge (Hamburg, Germany) for 15 min at 6 °C. The protein-rich supernatant was decanted and directly used for further characterization or emulsification.

2.3. Characterization of the protein-containing supernatant

2.3.1. Protein content

The protein content was determined according to the photometric method of Bradford (1976). For this purpose, 1 mL of Quick Start Bradford 1x Dye Reagent (Bio-Rad Laboratories Inc., Hercules, CA, USA) was mixed with 20 µL of the sample (diluted if necessary), and the extinction of the sample was determined at 595 nm after 15 min of incubation using the Evolution 201 UV–vis-spectrophotometer (Thermo Scientific, Waltham, MA, USA). Using a calibration based on bovine serum albumin (BSA) (Carl Roth GmbH + Co. KG, Karlsruhe, Germany). THe protein content was determined in BSA-equivalents.

2.3.2. Differential scanning calorimetry

To investigate the denaturation behavior of yeast proteins, 10–15 mg of the supernatant were sealed in small aluminum pots. Together with a reference pot, containing air, the samples were heated from 20 to 95 °C with a rate of 5 K min^{-1}, using the Perkin Elmer DSC 8000 (Waltham, MA, USA). In the thermogram of the measurement, endothermic peaks indicate the temperature at which the native protein structure is lost due to denaturation processes. Peak temperatures were read from each thermogram and averaged to determine denaturation temperatures.

2.3.3. pH value and electrical conductivity

The multimeter edge HI2020-02 from HANNAH Instruments (Vöhringen, Germany) was used to measure pH value and electrical conductivity. The pH value was adjusted to the desired value using 1 M HCl and 10 M NaOH (both Carl Roth GmbH + Co. KG).

2.3.4. Zeta potential and hydrodynamic diameter

The zeta potential and the average hydrodynamic diameter of the proteins were measured at different pH values with a Nanopartica SZ-100Z (Horiba Scientific, Kyoto, Japan). To measure the zeta potential, the supernatant was diluted 1:5, the desired pH value was adjusted and the electrophoretic mobility was measured using laser doppler electrophoresis technique at 25 °C. The zeta potential was calculated from the electrophoretic mobility using the Smoluchowski model by the in-built software. The measurement was carried out 10 times for each pH value for three different solutions.

The average hydrodynamic diameter, hereinafter referred to as hydrodynamic diameter, was measured by diluting the supernatant with water after pH adjustment to a concentration of 0.015 wt%. The diluted protein solution was swirled on the shaker at room temperature for 90 min to hydrate the proteins. Since aggregates with a size of more than 1 μm disturb the measurement because sedimentation superimposes brownian molecular motion, the samples were filtered through a polyethersulfone filter (PES) with a pore size of 1 μm before the measurement (J.T. Baker, Radnor, PA, USA). For each measuring point, 10 runs were carried out in 3 solutions each with a running time of 15 s. The refractive index required for the measurement was set to 1.450 for yeast protein (Lee et al., 2024) and 1.333 for water.

2.3.5. SDS-PAGE

Bi-distilled water was used to carry out the SDS-PAGE. For the running buffer, 15.15 g Tris (tris-(hydroxymethyl)-aminomethane), 72.00 g glycine, and 5.00 g SDS (sodium dodecyl sulfate) (all Carl Roth GmbH + Co. KG) were dissolved in 500 mL water. The following material from Bio-Rad Laboratories Inc. (Hercules, CA, USA) was used: Mini-PROTEAN TGXTM gels, Precision Plus Protein Standards All Blue, Coomassie Brilliant Blue R-250 Staining Solution, Coomassie Brilliant Blue R-250 Destaining Solution and 4x Laemmli Sample Buffer. All samples were diluted 1:8.5 with the sample buffer and heated for 5 min in a water bath at 95 °C. 10 μL of the diluted and heated sample were transferred into the gel wells. Electrophoresis was carried out at 200 V for approximately 30 min in the Mini-PROTEAN Tetra Cell from Bio-Rad Laboratories Inc. (Hercules, CA, USA). The gels were washed three times with bi-distilled water and placed in the staining solution on the shaking table for one hour. The gels were again washed three times and placed in a destaining solution for one hour before they were photographed. Only one determination was made for the SDS-PAGE.

2.3.6. Particle size distribution

The supernatant was adjusted to pH 3, 5, and 7, respectively, and left to stand for 2 h to investigate the protein aggregation. The highly diluted samples were measured by static laser light scattering (SLS) in the standing measuring cell of the particle analyzer (LA-950 from Horiba, Microtac Retsch GmbH, Haan, Germany). A refractive index of 1.450 (Lee et al., 2024) was used for yeast protein and 1.333 for water. The results are presented as the volumetric cumulative size distribution Q_3 or its 90th percentile ($x_{90,3}$). Microscope images were taken with an Eclipse LV100ND microscope from Nikon (Shinagawa, Tokyo, Japan).

2.4. Emulsion preparation

To produce emulsions, the supernatant was adjusted to the desired pH and used as continuous phase. Rapeseed oil (B. Schell, Lichtenau (Baden), Germany) was used as the disperse phase in varying concentrations. The total weight of all emulsions produced was 150 g. The oil was added while using an Ultra Turrax T 25 digital (IKA, Staufen im Breisgau, Germany) at 12,000 rpm (7.85 m/s) for 30 s. The emulsion premix was directly transferred to the high-pressure homogenizer and emulsified at 400 bar for one pass (Microfluidizer M-110EH with a y-reaction chamber, Microfluidics Cooperation, Newton, MA, USA).

For the emulsions with varying pH values, the supernatant after pH adjustment was used as described above. For the emulsion with varying oil content, the supernatant was partially diluted with water (with a correspondingly adjusted pH value). In other words, only for the emulsion with 50 wt% oil, the supernatant was used at its initial concentration. For the emulsions with lower oil content water was added to the supernatant to produce the continuous phase, whereby the protein mass in each emulsion was kept constant.

2.5. Emulsion characterization

2.5.1. Droplet size distribution

The determination was carried out analogously to the measurement of the particle size distribution. Deviating from this, the flow measuring cell was used. The refractive index for oil was 1.470 and for water 1.333. After mixing the sample by gently shaking, it was added to the measuring cell.

2.5.2. Shear rheology

To determine the viscosity of the emulsions, the Physica MCR 301 rotational rheometer was used (Anton Paar, Graz, Austria). For the liquid samples (2–10 wt% oil), a double gap geometry (DG 26.7) was used, while the emulsions with 30 and 50 wt% oil, which had a more pasty consistency, were measured using a plate–plate geometry (PP 25/SS). All measurements were conducted at 25 °C and at a shear rate that was increased logarithmically from 1 to 1000 s^{-1}, recording six measurement points per decade.

2.6. Statistical analysis

Unless otherwise stated, measurements were performed in triplicate. Statistical analyses were performed using Origin 2020 (OriginLab Corp., Northampton, MA, USA). The results in this work are presented as means ± standard deviation.

3. Results and discussions

3.1. Characterization of the protein-containing supernatant

The supernatant used for emulsification after cell disruption included all the water-soluble components contained in the yeast cubes: Mainly proteins from inside the cell, but also salts from the cytoplasm. In addition to these components from the interior of the cells, water-soluble residues from the fermentation could have been also present in the supernatant, which could have been involved in emulsion stabilization. Meirelles, Da Cunha, and Gombert (2018) has already shown that at the interface with oil, the wash water after washing yeast cells has a reduced interfacial tension compared to pure water. However, no additional washing step was carried out for this work, as it was assumed that the observed emulsion-stabilizing effect is mainly due to the proteins. The results of the various characterization methods of the supernatant with all soluble components are presented below.

The pH value of the supernatant increased from 4.62 ± 0.03 to 5.46 ± 0.01 due to cell disruption. The starting pH value depended on the fermentation conditions. Since yeast cells reproduce better at lower pH values and as only water is removed after fermentation to produce cubes of fresh yeast, the pH value is slightly acidic when the yeast cells are re-suspended in water (Salari & Salari, 2017). The increase in pH during cell disruption in this study was because the cytoplasm was released and the intracellular pH of yeast cells is between pH 6 and 7 (Babayan, Bezrukov, Latov, Belikov, Belavtseva, & Titova, 1981). Thus, the increase in pH was an indication that cell disruption was successful.

The demineralized water that was used to prepare the cell suspension had an electrical conductivity of 0.01 mS cm^{-1}. The conductivity of the supernatant after cell disruption and centrifugation was

2.89 ± 0.04 mS cm^{-1}. The cytoplasm of microorganisms contains relatively high amounts of electrolytes: Hölzel and Lamprecht (1992) published a conductivity for the cytoplasm of approximately 5.55 mS cm^{-1}. When the cells were broken down, these electrolytes were released from the cytoplasm, and the conductivity of the suspension, and thus of the supernatant, increased.

The protein content in the supernatant that could be achieved at 1200 bar and one pass in the high-pressure homogenizer was 9.85 ± 0.84 mg BSA-equivalent per mL. It is assumed that these were mainly proteins from inside the yeast cell. However, it could not be ruled out that the high shear forces in the high-pressure homogenizer caused mannoproteins to be sheared off and pass into the supernatant instead of being separated with the cell walls during centrifugation (Narsipur et al., 2024).

Using differential scanning calorimetry (DSC), two denaturation temperatures were determined for the protein solution. An example thermogram for the evaluation of the peaks can be seen in Fig. 9 in the supplementary materials. The first peak was at 39.23 °C ± 3.94 °C and the second at 82.13 ± 4.73 °C. This is in agreement with earlier studies of Otero et al. (2000) that report a denaturation temperature of 66.66 °C for whole yeast cells and denaturation temperatures between 46 and 70 °C for isolated protein fractions from disrupted yeast cells. When cells are disrupted, the protective effect of the cellular matrix and of cell components such as nucleic acids and polysaccharides is lost causing a lower denaturation temperature of several protein fractions (Otero et al., 2000). In this study, cell disruption was performed using high-pressure homogenization. The cell suspension was pre-cooled prior to processing, which effectively limited temperature increase during homogenization. Temperature monitoring confirmed that values consistently remained well below 30 °C. Since the first denaturation event, as indicated by the thermogram, occurred at approximately 40 °C, heat-induced denaturation during cell disruption can be excluded. Accordingly, the proteins in the resulting extracts were assumed to be unaffected by thermal denaturation.

3.2. Characterization of the supernatant after pH adjustment

3.2.1. Electrical conductivity

According to the DLVO theory, the stability of an emulsion depends on the strength of the repulsive and the attractive forces between the droplets. Their relation is influenced, among others, by the charge of the droplets, more precisely by their zeta potential (Verwey, 1947). Nevertheless, the stability of an emulsion can be improved or worsened by ionic emulsifiers or by ions in the continuous phase, which shield charges on the droplet surface (Köhler & Schuchmann, 2012). Therefore, adjusting the salt content of the continuous phase can be a measure to influence emulsion stability. However, the investigation of salt reduction and addition goes beyond the scope of this study. Thus, the effect of the salt content, measured as conductivity in the solution, should be monitored even if not explicitly studied.

The conductivity of the continuous phase used was influenced by both the presence of ions from the cytoplasm of the cells (see chapter 3.1) and the pH adjustment because the addition of HCl and NaOH led to a change in the salt content. The electrical conductivity was therefore measured in the supernatant at different pH values. Without pH adjustment (pH 5.46 ± 0.01) the electrical conductivity was 2.89 ± 0.04 mS cm^{-1}. The pH adjustment increased the conductivity in all cases. When reduced to pH 3 the conductivity increased to 5.71 ± 0.01 mS cm^{-1}, at pH 5 it also increased but only to 3.21 ± 0.04 mS cm^{-1}. After adjusting to pH 7 the conductivity was 3.42 ± 0.03 mS cm^{-1}.

As expected the conductivity was the highest at pH 3, followed by pH 7 and 5. This can be explained by the fact that the amount of HCl or NaOH required to adjust the pH value is greatest at pH 3, followed by pH 7 and 5. These values are comparably high for food emulsions. For example, the conductivity of beverage emulsions is typically less than 0.1 mS cm^{-1} (Bindereif, Karbstein, & van der Schaaf, 2023).

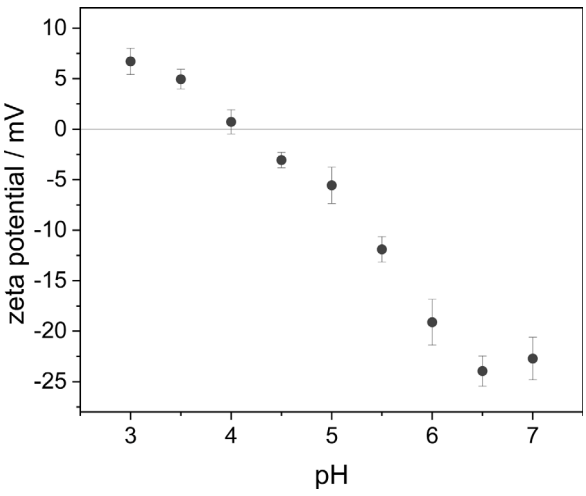

Fig. 1. Zeta potential of the supernatant after cell disruption and centrifugation at different pH values.

3.2.2. Zeta potential

In this study, the zeta potential of the supernatant was measured at different pH values between pH 3 and 7 to determine the isoelectric point (IEP) of the proteins. The data are presented in Fig. 1.

The measured surface charges exhibited a typical curve progression for proteins: At low pH values, the surface charge was positive, for instance, at pH 3, the surface charge was approximately 7 mV. The zeta potential reached 0 mV at about pH 4 indicating the IEP of the proteins in the supernatant. As the pH value increased, the surface charge became more negative: At pH 5, the surface charge was about −6 mV, and at pH 7, it was approximately −22 mV.

The absolute values of the measured zeta potentials were lower than described in the literature: In Lee et al. (2024), for example, the zeta potential is 30 mV at pH 3 and −30 mV at pH 7. This can be explained by the fact that the measurement conditions, such as the ionic strength, are not always comparable. The ionic strength also differed between the measuring points within this study due to pH adjustment. The addition or presence of ions could have shielded the intrinsic charges of the proteins and thus reduced the surface charge and possibly shift the measured IEP of the proteins from the real one (Kampen, 2005). In Lee et al. (2024), the ionic strength is also not buffered for different measured values, and an IEP for yeast proteins of 4.4 is determined. In addition to the deviation of the ionic strength, these differences could lie in the type and extent of protein processing before the determination. This study examined the supernatant after cell disruption which thus contains a mixture of all soluble proteins and cell components whereas Lee et al. (2024) used a protein isolate: Not all protein fractions may have precipitated in the isolation process. Different protein fractions have varying molecular compositions and thus different surface charges. For example, Haehn (1952) differentiated between the two fractions yeast albumin with an IEP of 4.59, and zymocasein, whose IEP is 3.6. This explains the deviations in surface charge and isoelectric point between several studies with differently processed raw materials.

3.2.3. Size distribution of soluble and aggregated proteins

When assessing emulsion stabilizing properties, it is important to examine the size and aggregation behavior of proteins, as this influences the diffusion to and adsorption at the interface and defines the contribution of the proteins to the steric stabilization of the droplets (Köhler & Schuchmann, 2012). Therefore, the hydrodynamic diameter of the proteins and the size of formed aggregates was monitored.

Generally yeast proteins are poor soluble and they tend to aggregate (Ma et al., 2024; Otero et al., 2000). A possible cause could be

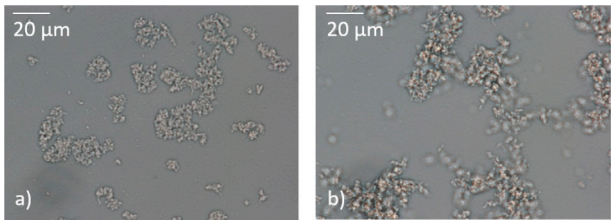

Fig. 2. Protein aggregates after adjusting the pH value in the supernatant to pH 3 (left) and pH 5 (right).

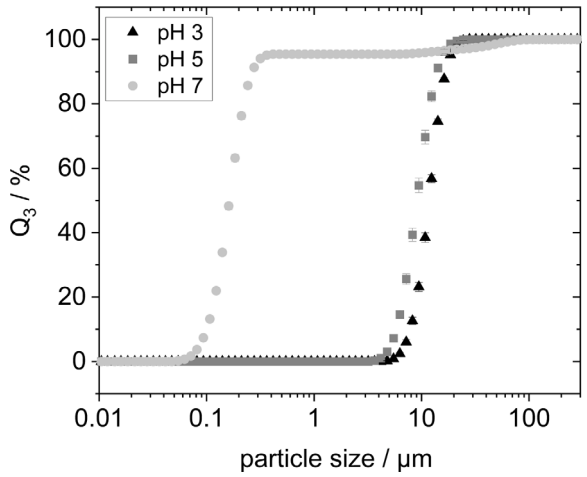

Fig. 3. Particle size distribution of the protein aggregates that precipitated from the supernatant after adjustment of the pH value to 3, 5 and 7.

the high proportion of hydrophobic amino acids or the very ordered structure with the most common being beta-sheet, followed by alpha-helix (Ma, Sun, et al., 2023; Ma, Xia, et al., 2023). Proteins with a beta-sheet structure usually exhibit a high surface hydrophobicity and tend to form water-insoluble aggregates (Ma, Xia, et al., 2023). It is generally known that proteins have the lowest solubility at their isoelectric point. This is because the repulsion between protein molecules due to the neutral net charge is very low, they can get closer, and aggregate (Xia, 2007).

The yeast proteins at different pH values were examined under the microscope to examine aggregates that might have formed. The images of the proteins at pH 3 and 5 can be seen in Fig. 2. At pH 7, no precipitate was visible, the protein was almost completely in solution (picture not shown). In Fig. 2 it can be seen that the proteins have aggregated into larger structures at both pH values. The microscope images give the impression that the aggregates were larger at pH 5. To obtain a quantitative statement, the size of the aggregates was determined using static laser light scattering (SLS). The results of this measurement can be seen in Fig. 3. The figure shows that at pH 3 and 5 the particle size distribution was monomodal. At pH 3, the particles had a size between 5 and 25 µm. At pH 5, the particles were slightly smaller with 4–20 µm. The quantitative measurement shows that the aggregate sizes hardly differed from each other at pH 3 and pH 5.

At pH 7, the particle size distribution was bimodal with most of the particles being in the range of 0.05 to 0.3 µm and only a small proportion of particles being much larger, namely between 5–80 µm.

One reason for the aggregation at pH 3 and 5 could be the proximity to the IEP and thus the poor solubility of the proteins due to the lack of surface charge. Both pH values deviated by the same amount from the determined IEP (approx. pH 4, s. chapter 3.2.2). In Lee et al. (2024), the lowest solubility of the proteins is also determined at pH 4 and pH 5. Lee et al. (2024) determines that the solubility at pH 3 is with 40 % twice as high as at pH 7 (20 %). This does not correspond to the observations made in this study, where the proteins were still in solution at pH 7 but precipitated at pH 3. Instead, the presented results are in line with Pacheco and Sgarbieri (1998), who after isoelectric precipitation also finds a much higher solubility at pH 7 than at pH 3.

According to Kinsella and Shetty (1978), protein solubility in this study was poorer at pH values below the IEP. One reason for the precipitation in acidic conditions at pH values away from the IEP could be that acid denaturation and thus molecular unfolding occurred at these pH values. Due to this unfolding, the denaturation could have led to exposing hydrophobic side chains from the interior of the protein, increasing the hydrophobicity of the proteins and decreasing their solubility (Jiang, Chen, & Xiong, 2009; Kinsella & Shetty, 1978; Ma, Xia, et al., 2023; Pauly, Heinrichs, & Luck, 1996). In addition to increasing hydrophobicity, the ionic strength of the medium also influenced the aggregation behavior of proteins at pH 3: According to Pauly et al. (1996), a higher ionic strength of the solvent leads to increased aggregation reactions after unfolding due to temperature-induced denaturation. As described in chapter 3.2.1, at pH 3 the ionic strength was increased by the pH adjustment. Both acid denaturation and higher ionic strength could have been reasons for the slightly larger aggregates at pH 3 than at pH 5.

Despite the precipitation and aggregation of a part of the proteins, a significant proportion remained in the solution, especially at pH 7. The hydrodynamic diameter (D_h) of these soluble proteins was determined using dynamic light scattering (DLS). At pH 3, the dissolved proteins had a hydrodynamic diameter of 97.76 ± 4.04 nm. At pH 5, this value was 104.23 ± 5.9 nm.

In contrast, at pH 7 the hydrodynamic diameter of the proteins was much larger (D_h = 151.3 ± 9.68 nm). This means that the hydrodynamic diameter of the proteins was significantly larger at this pH value than at pH 3 and 5 and was in line with the size obtained by SLS (see Fig. 3). The reason for this could be the increased charge of the molecule, as detected by measuring the zeta potential. In addition to the increased repulsive intermolecular forces that prevent aggregation, the charges also influence the conformation of the molecules: Electrostatic intramolecular repulsion loosened the protein structure and increased the D_h. This loosened structure made it easier for water molecules to penetrate the otherwise more compact molecular structure and the molecule tended to remain in solution instead of precipitating (Kinsella & Shetty, 1978).

3.2.4. SDS-PAGE

SDS-PAGE, buffered by TRIS, was performed to investigate possible differences in the binding form between the protein molecules during the previous formation of aggregates in the supernatant at different pH values. If covalent bonds were to form between individual molecules that were not reversible under SDS-PAGE conditions, this would have been reflected in the presence of bands at higher molecular weights. Fig. 4 shows the gel on which the supernatants without pH adjustment and after adjustment to pH 3, 5, and 7 were applied before electrophoresis together with a molecular weight standard.

The supernatant without pH adjustment showed several protein bands (lane a): At the level of the 10 kDa marker, an intensely colored band can be seen. This suggests that the solution contained small peptides. However, it is unclear whether these peptides were building blocks for larger proteins in the cell or degradation products of cell proteins after cell lysis by the cell's enzymes. Proteolytic enzymes are found in the vacuole of yeast cells. During the life cycle of a cell, they work only slowly but the protein degradation is accelerated when the cells are destroyed, e.g. by cell disruption (Behalová & Beran, 1979). Above 10 kDa, various blocks of bands can be observed up to a size of 75 kDa. The most noticeable band was at 35 kDa. Several of the observed blocks of bands are also found by Lee et al. (2024) for YPI. However, interestingly, the intense band at 10 kDa is not observed by Lee. This difference may be explained by the fact that Lee et al. (2024)

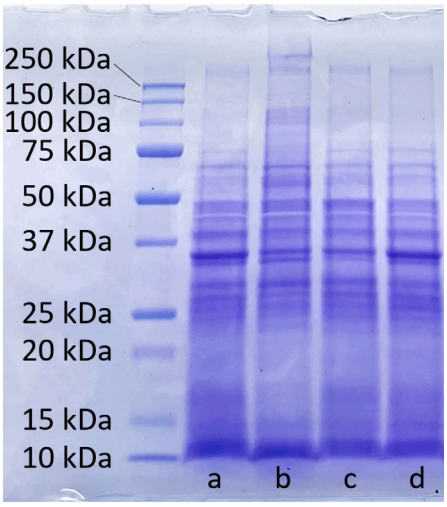

Fig. 4. Molecular weight distributions of yeast proteins, determined by (SDS-PAGE) (a) supernatant after cell disruption and centrifugation and after adjustment to (b) pH 3, (c) pH 5 and (d) pH 7.

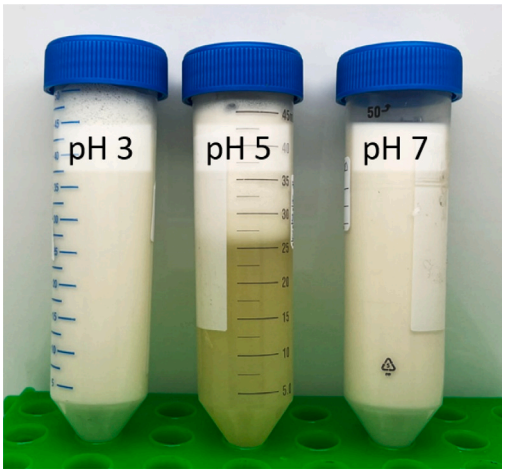

Fig. 5. Differently stable emulsions on the day of preparation from 5 wt% rapeseed oil and 1 wt% yeast proteins with pH values in the continuous phase of 3, 5, and 7, prepared with high-pressure homogenization at 400 bar.

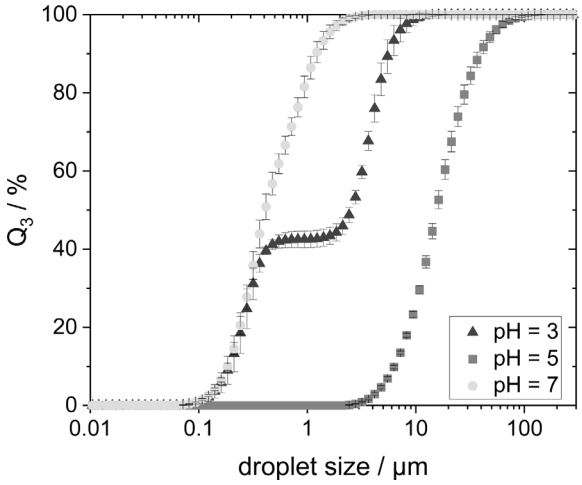

Fig. 6. Droplet size distributions of three emulsions, prepared with 5 wt% rapeseed oil and 1 wt% yeast proteins with high-pressure homogenization at 400 bar at pH 3, 5 and 7.

investigates a protein isolate prepared by isoelectric precipitation. Even if small peptides had been present, they would likely remain in solution when the pH was adjusted to the IEP and would not have been separated when the precipitate was centrifuged.

The pH adjustment in this study resulted in the following: The pH adjustment to 5 or 7 (lanes c and d) did not lead to any differences in the visual bands indicating that the molecular weight of the protein fractions did not change. In contrast, changes did occur after adjusting the pH of the supernatant to 3 (lane b). Here, the bands in the range from 12–17 kDa and at 35 kDa became weaker whereas the two bands between 50 and 70 kDa were more intense. An additional coloration can be seen between 75 and 150 kDa as well as in the area of the gel pockets at approx. 250 kDa. This indicates that larger proteins (> 75 kDa) had formed from smaller ones (35 kDa and smaller) via covalent bonds. The occurrence of a blue band at the well of lane b indicates that protein aggregates had formed that were even too large to enter the gel.

The increase in molecular weight at pH 3 could have occurred because denaturation in acidic conditions led to the release of hydrophobic and reactive groups that were previously hidden within the globular protein. Then, protein molecules covalently crosslinked via disulfide bonds which was reflected in an increased molecular weight (Jiang et al., 2009). Although aggregation of the proteins was observed at pH 5 (see Fig. 2), this was not reflected by a higher particle size using light scattering (see Fig. 3) or a larger molecular weight units in the SDS-PAGE. The aggregation of proteins at this pH value seems to have been reversible under the prevailing conditions of particle size measurement by light scattering and of SDS-PAGE.

3.3. Influence of pH value on the emulsion stability

To investigate the effect of the pH value on the emulsion stabilizing properties of yeast proteins and to gain an overall deeper insight into the stabilization mechanism of the proteins, 5 wt% oil in water emulsions were prepared at different pH values.

The emulsions produced showed very different results (s. Fig. 5): The emulsion at pH 3 appeared white and homogeneous and retained this state even during storage for more than four weeks.

At pH 5, directly after production, strong creaming occurred to such an extent, that a yellowish-colored aqueous layer remained at the bottom. All oil droplets accumulated in the top region of the tube. However, the emulsion did not break even after four weeks of storage as was proven by the redispersion of the droplets after shaking (image not shown). At pH 7, the emulsion appeared just as homogeneous as at pH 3 immediately after production, but partitioning occurred after four weeks (pictures not shown).

To explain the observed differences, the droplet size distributions (DSD) were measured using static light scattering (see Fig. 6). As the algorithm for calculating the particle size of this measurement method assumes detected objects to be solid spheres, it is not possible to judge from the droplet size distribution alone whether it is a large particle or an aggregate consisting of small particles. Therefore, the samples were additionally examined using light microscopy in order. The microscope images are shown in Fig. 7 and are discussed together with the DSD.

Rather different emulsion microstructures were identified: At pH 3, a bimodal droplet size distribution was detected. Microscopy helped to identify the fraction of smaller droplets as free flowing droplets. In contrast, the fraction of larger droplets were loosely arranged flocs, detected by SLS as larger droplets.

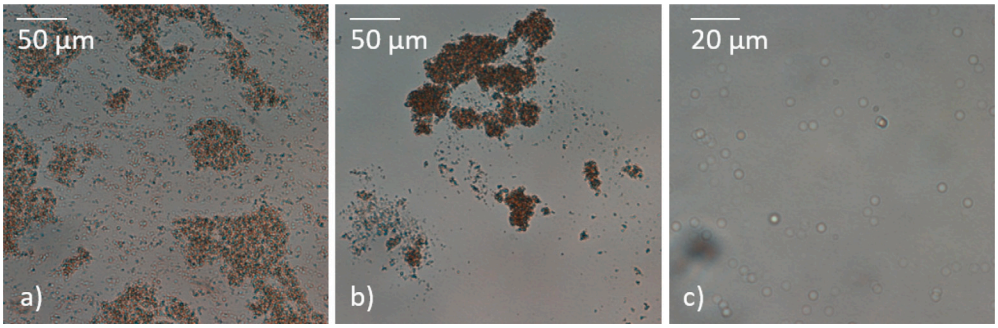

Fig. 7. Microscope images of emulsions prepared with high-pressure homogenization at 400 bar, 5 wt% oil and 1 wt% oil at (a) pH 3, (b) pH 5 and (c) pH 7.

The free-flowing droplets were about 0.1–0.5 µm in size, while the flocs ranged from 1.5–15 µm. The flocs in the microscope image appear larger than those measured using SLS. Apparently, the loose structure of the flocs allows them to be broken down into smaller units by stirring during measurement. At pH 5, the distribution was monomodal and showed overall much larger measured sizes, ranging from 2.5 to 125 µm. Again flocs could be seen under the microscope, this time more compact. At pH 7, the smallest droplet sizes were measured. The distribution was monomodal with droplet sizes in the range from 0.1 to 4 µm. By microscopy, these droplets could be identified as free-flowing.

It is assumed that a different behavior of the proteins was the reason for the different structuring of the oil phase in the emulsions. In all emulsions prepared at pH 3, 5, and 7, very small oil droplets could be stabilized by the proteins used, and in no case the emulsion did break. However, at different pH values, the small oil droplets were arranged in different structures: At pH 7, the proteins were mostly in dissolved form, and as described in chapter 3.2.3, no protein aggregates could be observed under the microscope. The zeta potential of about −22 mV indicates that the surface of the protein was charged. But also repulsive charges inside the folded proteins could lead to a loosened structure (see the results of the hydrodynamic diameter in chapter 3.2.3). Due to the water-soluble properties and at the same time due to exposed hydrophobic areas from the interior of the loosened protein, at pH 7 the proteins contributed to the stabilization of the oil droplets. It is assumed that this stabilization was due to the reduction of the interfacial tension through the amphiphilic structure of the proteins, the formation of a steric barrier around the droplet, and at the same time due to electrostatic forces that prevented the droplets from approaching each other and thus preventing flocculation.

In contrast at pH 5 the stabilization of the emulsion was significantly worse: The microscope images showed that the oil was present in finely distributed drops even at this pH value. However, they aggregated into large flocs, presumably through bridging flocculation (s. Fig. 7b). The aggregation into compact flocs increased the creaming speed of the droplets enormously, which led to the creaming of the flocs and partitioning of the emulsion immediately after their production (Damodaran, 2005; Dickinson, 2010). This behavior can be explained as follows: Due to the poor solubility near the IEP and the aggregation of proteins, the molar concentration of proteins acting as surfactant particles decreased while the size of the interface remained the same. The aggregates could still attach to oil droplets with their hydrophobic areas, but the reduced concentration led to bridging flocculation between the oil droplets. A characteristic of such bridging flocculation is rather strong bonds between the oil droplets and very compact structures of the flocs (Dickinson, 2010, 2013). The flocculation is promoted by low electrostatic repulsion which makes it possible for droplets to approach each other closer (Köhler & Schuchmann, 2012; Pearce & Kinsella, 1978). At pH 5, the measured zeta potential was only −6 mV which was not sufficient to stabilize free-flowing droplets. Typically, an emulsion is considered stable if the absolute value of the zeta potential is greater than 30 mV (Köhler & Schuchmann, 2012).

At pH 3 the emulsion remained externally homogeneous even over a longer period. Probably due to the aggregation of the protein molecules and the low zeta potential at this pH value (comparable with pH 5), some of the oil droplets agglomerated into flocs like at pH 5. In contrast to pH 5, the formed flocs appeared looser and less compact (s. Fig. 7a) and some oil droplets still existed as individual drops. Presumably, the individual droplets and the looser structuring of droplet flocs resulted in a significantly lower creaming speed compared to pH 5 which prevented partitioning of the emulsion. One possible explanation for the presence of individual droplets and the looser structure could be that denaturation and thus unfolding of the proteins occurred in acidic conditions. The unfolding exposed hydrophobic areas from the interior of the proteins (Jiang et al., 2009; Jiang, Wang, & Xiong, 2018). This could have led to hydrophobic aggregation, but also to better adsorption to the interface and more efficient stabilization of small droplets (Jiang et al., 2018). In Ma et al. (2024), it is shown that the emulsifying ability of yeast proteins increases through ultrasound treatment, because of the release of hydrophobic groups. An indication of occurring acid denaturation and the resulting unfolding of proteins in this study was the formation of covalent bonds at pH 3 as could be seen using SDS-PAGE (s. chapter 3.2.4). By unfolding the proteins, not only hydrophobic groups were exposed from the interior, but also reactive groups that could form disulfide crosslinking (Jiang et al., 2009). As already mentioned, the unfolded proteins could better adsorb to the oil interface due to the additionally exposed hydrophobic groups. As at pH 5, also at pH 3 too low a protein concentration or too low electrostatic repulsion between the droplets probably could have led to the aggregation of some oil droplets into larger flocs. In contrast to pH 5, the observed flocs had a looser and less densely packed structure. The loosened molecular structure is expected to be the cause of this. The loosened proteins could increase the steric barrier formed around the droplets. In addition to the unfolding by acid denaturation, swelling of yeast cysteine under acidic conditions could also have been a reason for the better hydrated proteins and therefore the loosened structure of the flocs (Haehn, 1952). But also the salt-in-effect could be an explanation for the unfolding of the proteins (Timasheff & Arakawa, 1988). At pH 3 the ionic strength was higher compared to the other pH values investigated and could have caused increased unfolding.

3.4. Influence of oil content

So far, results for emulsions with 5 wt% disperse phase have been shown and discussed. In the food sector, however, there is a wide range of applications with sometimes significantly higher oil contents.

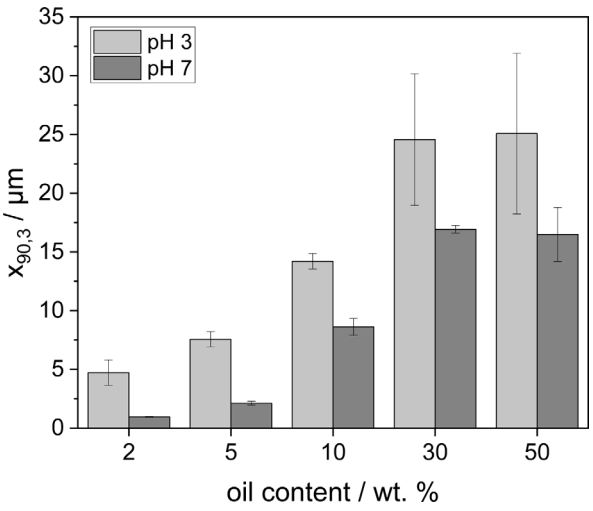

Fig. 8. $x_{90,3}$-values of emulsions, prepared with 2–50 wt% rapeseed oil and a constant protein concentration of 0.5 wt% with high pressure homogenization at 400 bar at pH 3 and pH 7.

Therefore, the suitability of yeast proteins to stabilize emulsions with a dispersed phase content of between 2 and 50 wt% was also investigated at three different pH values. A stable emulsion could not be produced at any pH value with oil contents above 50 wt% under the conditions listed here. Immediately after production, emulsions with oil contents higher than 50 wt% appeared inhomogeneous and an oil and water phase was formed, with large lumps, presumably proteins, floating within the oil phase (pictures not shown).

For all emulsions produced at pH 5, partitioning occurred immediately after production or at least after a few hours at higher oil contents. For this reason, these emulsions were not evaluated further.

The viscosity of the protein solution hardly differed at all three pH values, but as expected, the oil content strongly influenced emulsion viscosity. As an example, viscosity data of emulsions prepared at pH 3 are shown in Fig. 10 in the supplementary materials. The figure shows that the measured viscosities of the emulsions prepared at pH 3 increased with increasing oil content, which was expected (Barnes, 2000). This trend was also visible for the emulsions prepared at pH 5 and 7 (data not shown). At low oil content (2 wt%), emulsions had a watery texture, whereas at high oil content (50 wt%) the emulsion had a cream cheese-like texture (s. Fig. 11 in the supplementary materials). All emulsions showed shear thinning behavior as expected for emulsions and that was more pronounced with higher oil content (Mezger, 2023).

Fig. 8 shows the $x_{90,3}$-values of the emulsions prepared at pH 3 and 7. For both samples, an increase in the $x_{90,3}$-value can be seen with increasing oil content up to 30 %. Even with a further increase in oil content, the $x_{90,3}$ value did not increase any further.

In an emulsion made at pH 7 with an oil concentration of 2 wt%, the $x_{90,3}$-value was approx. 1 µm. Up to an oil concentration of 30 wt%, the $x_{90,3}$-value increased to 16.9 ± 0.3 µm. Under the microscope, it was seen that the increasing $x_{90,3}$-value at pH 7 in 8 was due to coalescence, but not flocculation (s. Fig. 12 in the supplementary materials). A possible cause for the coalescence observed at pH 7 could be that with increasing oil content, but constant protein concentration, there were no longer enough emulsifier molecules for the newly created interfaces and coalescence occurred as long as droplet surfaces were not completely occupied. From a certain droplet size, the emulsifier molecules were sufficient to stabilize the interface and no further coalescence took place. This phenomenon is called limited coalescence (Arditty, Whitby, Binks, Schmitt, & Leal-Calderon, 2003).

At pH 3 the $x_{90,3}$ of the emulsion with 2 wt% oil was 4.7 ± 1.1 µm. At an oil concentration of 30 wt% the $x_{90,3}$-value was 24.6 ± 5.6 µm. Thus, the $x_{90,3}$-values of the emulsions at pH 3 were significantly higher than those at pH 7, which was due to the formation of flocs. The number of individual droplets decreased with increasing oil content and from an oil content of 10 wt% the curve was no longer bimodal (data not shown). The increase in the $x_{90,3}$-value at pH 3 was due to both, coalescence and the formation of larger flocs as could have been seen under the microscope (pictures not shown). Possible mechanisms are, as already explained for pH 3 in chapter 3.3, the too-low protein concentration due to aggregation of the molecules near the isoelectric point and the resulting flocculation of the oil droplets, stabilized by protein aggregates. The higher the oil content, the more bridging flocculation took place, but also coalescence played a role at pH 3 and at the same time higher oil contents, as explained in this chapter for pH 7.

One reason why the droplet size did not increase further at 50 wt% oil at both pH values investigated, even if the emulsifier-to-oil-ratio was even lower, could be that the viscosity of the emulsions increased significantly with increasing oil content. On the one hand, this reduced the creaming speed of the oil droplets according to Stokes (Köhler & Schuchmann, 2012). On the other hand, reduced droplet mobility decreased the coalescence probability of the droplets, which reduced coalescence processes.

Even with high oil contents, the emulsions at pH 3 were more stable than at the other two pH values considered. At both pH 5 and 7, there was significant partitioning within the emulsions within two weeks. At pH 3, however, only the emulsions at 5 and 10 wt% oil change externally: After 14 days, a small amount of aqueous phase could be seen below the emulsion. This is attributed to the better hydration of the protein molecules and thus the slower creaming speed at pH 3. At higher oil contents the viscosity of the emulsions was too high so the creaming rate of droplets and flocs was greatly slowed down.

4. Conclusion

Proteins extracted from the interior of yeast cells (*Saccharomyces cerevisiae*) by cell disruption via high-pressure homogenization were demonstrated to have the ability to stabilize oil in water emulsions. Oil contents of up to 50 wt% could be stabilized at pH 3 and 7. At these pH values, the emulsions appeared macroscopically homogeneous whereas at pH 5 partitioning occurred directly after emulsion preparation. A closer look at the droplet size distribution and microscopic images revealed differences in the structuring of the oil droplets, which were present either as single droplets (pH 7), densely packed droplet flocs (pH 5), or rather as loosely packed flocs (pH 3). The zeta potential, the aggregation of the protein molecules as well as the denaturation due to acid treatment, and through this the release of hydrophobic groups and a loosened protein structure are discussed as possible reasons for the differences in the oil structuring between the examined pH values.

CRediT authorship contribution statement

Laura Riedel: Writing – original draft, Visualization, Methodology, Investigation, Data curation, Conceptualization. **Ulrike S. van der Schaaf:** Writing – review & editing, Supervision, Project administration, Funding acquisition, Conceptualization.

Declaration of competing interest

The authors declare that they have no known competing financial interests or personal relationships that could have appeared to influence the work reported in this paper.

Appendix. Supplementary materials

See Figs. 9–12.

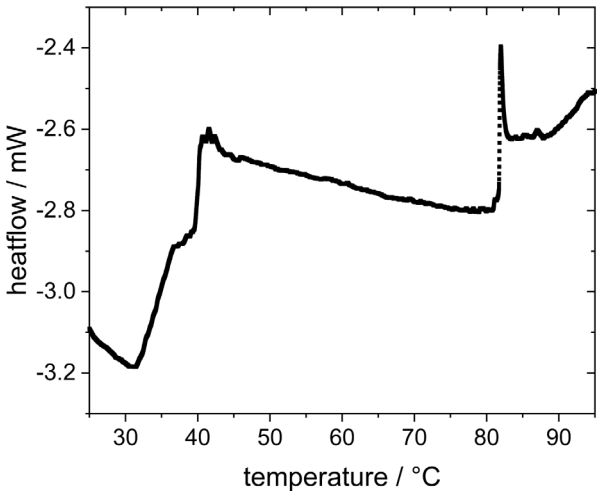

Fig. 9. Example of a thermogram for peak evaluation to determine the denaturation temperature.

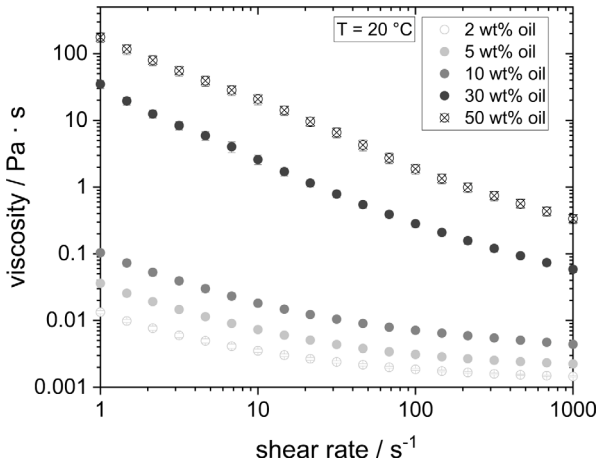

Fig. 10. Viscosity of emulsions prepared at pH 3 with high-pressure homogenization at 400 bar, varying disperse phase content between 2 and 50 wt% and constant protein concentration of 0.5 wt%.

Fig. 11. Cream cheese-like texture of the emulsion prepared at pH 3 with 50 wt% oil and 0.5 wt% protein with high-pressure homogenization at 400 bar.

Data availability

Data will be made available on request.

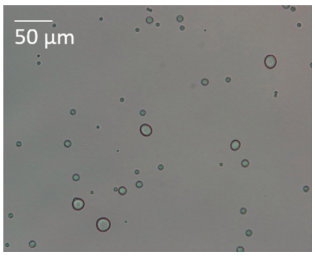

Fig. 12. Microscope image of the emulsion prepared with 50 wt% oil and a protein concentration of 0.5 wt% with high-pressure homogenization at 400 bar at pH 7.

References

Arditty, S., Whitby, C. P., Binks, B. P., Schmitt, V., & Leal-Calderon, F. (2003). Some general features of limited coalescence in solid-stabilized emulsions. *The European Physical Journal. E, Soft Matter*, *11*(3), 273–281.

Babayan, T. L., Bezrukov, M. G., Latov, V. K., Belikov, V. M., Belavtseva, E. M., & Titova, E. F. (1981). Induced autolysis of saccharomyces cerevisiae: Morphological effects, rheological effects, and dynamics of accumulation of extracellular hydrolysis products. *Current Microbiology*, *5*, 163–168.

Barnes, H. A. (2000). *A handbook of elementary rheology*. Aberystwyth: University of Wales Institute of Non-Newtonian Fluid Mechanics.

Barriga, J. A. T., Cooper, D. G., Idziak, E. S., & Cameron, D. R. (1999). Components of the bioemulsifier from s. cerevisiae. *Enzyme and Microbial Technology*, *25*, 96–102.

Behalová, B., & Beran, K. (1979). Activation of proteolytic enzymes during autolysis of disintegrated baker's yeast. *Folia Microbiologica*, *24*(6), 455–461.

Bergfreund, J., Bertsch, P., & Fischer, P. (2021). Adsorption of proteins to fluid interfaces: Role of the hydrophobic subphase. *Journal of Colloid and Interface Science*, *584*, 411–417.

Bindereif, B., Karbstein, H. P., & van der Schaaf, U. S. (2023). Sugar beet pectins for the formulation of dressings and soft drinks: Understanding the complexity of charged hydrocolloids in industrial food emulsions. *Food Hydrocolloids*, *135*, Article 108054.

Bradford, M. M. (1976). A rapid and sensitive method for the quantitation of microgram quantities of protein utilizing the principle of protein-dye binding. *Analytical Biochemistry*, *72*(1–2), 248–254.

Cameron, D. R., Cooper, D. G., & Neufeld, R. J. (1988). The mannoprotein of saccharomyces cerevisiae is an effective bioemulsifier. *Applied and Environmental Microbiology*, *54*(6), 1420–1425.

Cheng, T., Zhang, G., Sun, F., Guo, Y., Ramakrishna, R., Zhou, L., et al. (2024). Study on stabilized mechanism of high internal phase pickering emulsions based on commercial yeast proteins: Modulating the characteristics of pickering particle via sonication. *Ultrasonics Sonochemistry*, *104*.

Damodaran, S. (2005). Protein stabilization of emulsions and foams. *Journal of Food Science*, *70*(3), R54–R66.

Dickinson, E. (2010). Flocculation of protein-stabilized oil-in-water emulsions. *Colloids and Surfaces. B, Biointerfaces*, *81*(1), 130–140.

Dickinson, E. (2013). Stabilising emulsion-based colloidal structures with mixed food ingredients. *Journal of the Science of Food and Agriculture*, *93*(4), 710–721.

Firoozmand, H., & Rousseau, D. (2016). Microbial cells as colloidal particles: Pickering oil-in-water emulsions stabilized by bacteria and yeast. *Food Research International*, *81*, 66–73.

Gouel, C. G. (2017). Nutrition transition and the structure of global food demand. *International Food Policy Research Institute*, *1631*.

Haehn, H. (1952). *Biochemie der Gärung: Unter besonderer Berücksichtigung der Hefe*. Berlin: De Gruyter.

Hedenskog, G., & Mogren, H. (1973). Some methods for processing of single-cell protein. *Biotechnology and Bioengineering*, *15*, 129–142.

Heeres, A. S., Picone, C. S. F., van der Wielen, L. A. M., Cunha, R. L., & Cuellar, M. C. (2014). Microbial advanced biofuels production: overcoming emulsification challenges for large-scale operation. *Trends in Biotechnology*, *32*(4), 221–229.

Hölzel, R., & Lamprecht, I. (1992). Dielectric properties of yeast cells as determined by electrorotation. *Biochimica et Biophysica Acta*, *1104*(1), 195–200.

Jach, M. E., Serefko, A., Ziaja, M., & Kieliszek, M. (2022). Yeast protein as an easily accessible food source. *Metabolites*, *12*(1).

Jiang, J., Chen, J., & Xiong, Y. L. (2009). Structural and emulsifying properties of soy protein isolate subjected to acid and alkaline ph-shifting processes. *Journal of Agricultural and Food Chemistry*, *57*(16), 7576–7583.

Jiang, J., Wang, Q., & Xiong, Y. L. (2018). A ph shift approach to the improvement of interfacial properties of plant seed proteins. *Current Opinion in Food Science*, *19*, 50–56.

Kampen, I. (2005). *Einfluss der Zellaufschlussmethode auf die Expanded Bed Chromatographie* (Ph.D. thesis), Braunschweig: Technischen Universität Carolo-Wilhelmina zu Braunschweig.

Kim, W., Wang, Y., & Selomulya, C. (2020). Dairy and plant proteins as natural food emulsifiers. *Trends in Food Science & Technology*, *105*, 261–272.
Kinsella, J. E., & Shetty, K. J. (1978). Yeast proteins: recovery, nutritional and functional properties. *Advances in Experimental Medicine and Biology*, *105*, 797–825.
Köhler, K., & Schuchmann, H. P. (Eds.), (2012). *Emulgiertechnik: grundlagen, verfahren und anwendungen* (3. aufl. edn). Hamburg: Behr.
Lee, S., Kim, E., Jo, M., & Choi, Y. J. (2024). Characterization of yeast protein isolates extracted via high-pressure homogenization and ph shift: A promising protein source enriched with essential amino acids and branched-chain amino acids. *Journal of Food Science*.
Li, J., Karboune, S., & Asehraou, A. (2020). Mannoproteins from inactivated whole cells of baker's and brewer's yeasts as functional food ingredients: Isolation and optimization. *Journal of Food Science*, *85*(5), 1438–1449.
Ma, J., Sun, Y., Meng, D., Zhou, Z., Zhang, Y., & Yang, R. (2023). Yeast proteins: The novel and sustainable alternative protein in food applications. *Trends in Food Science & Technology*, *135*, 190–201.
Ma, C., Wan, Q., Song, J., Hao, T., Xia, S., Shen, S., et al. (2024). Ultrasound-assisted ph shift-induced interfacial remodeling for enhancing soluble yeast protein content: Effects on structure and interfacial properties of proteins under different treatment conditions. *Food Hydrocolloids*, *149*, Article 109521.
Ma, C., Xia, S., Song, J., Hou, Y., Hao, T., Shen, S., et al. (2023). Yeast protein as a novel dietary protein source: Comparison with four common plant proteins in physicochemical properties. *Current Research in Food Science*, *7*, Article 100555.
Meirelles, A. A. D., Da Cunha, R. L., & Gombert, A. K. (2018). The role of saccharomyces cerevisiae in stabilizing emulsions of hexadecane in aqueous media. *Applied Microbiology and Biotechnology*, *102*(7), 3411–3424.
Mezger, T. (2023). *Applied rheology: with joe flow on rheology road* (10. auflage edn). Graz: Anton Paar GmbH.
Moreira, T. C. P., da Silva, V. M., Gombert, A. K., & da Cunha, R. L. (2016). Stabilization mechanisms of oil-in-water emulsions by saccharomyces cerevisiae. *Colloids and Surfaces B (Biointerfaces)*, *143*, 399–405.
Narsipur, S., Kew, B., Ferreira, C., El-Gendy, R., & Sarkar, A. (2024). Emulsion stabilised by yeast proteins and biomass: a mini review. *Current Opinion in Food Science*, *57*, Article 101167.
Nasseri, A. T., Rasoul-Amini, S., Morowvat, M. H., & Ghasemi, Y. (2011). Single cell protein: Production and process. *American Journal of Food Technology*, *6*(2), 103–116.
Otero, M. A., Wagner, J. R., Vasallo, M. C., Garcıa, L., & Añón, M. C. (2000). Thermal behavior and hydration properties of yeast proteins from saccharomyces cerevisiae and kluyveromyces fragilis. *Food Chemistry*, *69*(2), 161–165.
Overbeck, A., Michel, S., Kampen, I., & Kwade, A. (2023). Temperature influence on the compression and breakage behaviour of yeast cells. *Letters in Applied Microbiology*, *76*(8).
Pacheco, M. T. B., & Sgarbieri, V. C. (1998). Hydrophilic and rheological properties of brewer's yeast protein concentrates. *Journal of Food Science*, *63*(2), 238–243.
Pauly, D., Heinrichs, M., & Luck, T. (1996). Evaluation of the denaturation kinetics of two differently prepared protein concentrates from bovine blood plasma. *Journal of Agricultural and Food Chemistry*, *44*(10), 3251–3256.
Pearce, K. N., & Kinsella, J. E. (1978). Emulsifying properties of proteins: Evaluation of a turbidimetric technique. *Journal of Agricultural and Food Chemistry*, *26*(3), 716–723.
Pittroff, M. (1993). *Mechanischer Aufschluß Von Mikroorganismen Iim Apparatevergleich Zwischen Rührwerkskugelmühle Und Hochdruckhomogenisator* (Dissertation), Karlsruhe: Universität Karlsrueh.
Qiao, Y., Xia, C., Liu, L., Tang, L., Wang, J., Xu, C., et al. (2022). Structural characterization and emulsifier property of yeast mannoprotein enzymatically prepared with a b-1, 6-glucanase. *LWT*, *168*, Article 113898.
Salari, R., & Salari, R. (2017). Investigation of the best saccharomyces cerevisiae growth condition. *Electronic Physician*, *9*(1), 3592–3597.
Sceni, P., Palazolo, G. G., Del Vasallo, M. C., Puppo, M. C., Otero, M. A., & Wagner, J. R. (2009). Thermal and surface behavior of yeast protein fractions from saccharomyces cerevisiae. *LWT*, *42*(6), 1098–1106.
Schachtel, A. P. (1981). Effects of preparative processes on the composition and functional properties of protein preparations from candida utilis. *Journal of Food Science*, *46*(2), 377–382.
Spalvins, K., Zihare, L., & Blumberga, D. (2018). Single cell protein production from waste biomass: comparison of various industrial by-products. *Energy Procedia*, *147*, 409–418.
Timasheff, S. N., & Arakawa, T. (1988). Mechanism of protein precipitation and stabilization by co-solvents. *Journal of Crystal Growth*, *90*(1–3), 39–46.
Tonnius, F. G. (1982). Verfahren zum herstellen von nucleinsäureaarmen proteinkonzentraten aus bäckerhefe. *ZFL*, *34*(1), 7–15.
Vananuvat, P., & Kinsella, J. E. (1975). Some functional properties of protein isolates from yeast, saccharomyces fragilis: J. agrie. food chem. 23, (4) 1975 613. *Journal of Agricultural and Food Chemistry*, *23*(4), 613–616.
Verwey, E. J. W. (1947). Theory of the stability of lyophobic colloids. *The Journal of Physical and Colloid Chemistry*, *51*(3), 631–636.
Xia, X. (2007). *Bioinformatics and the cell: modern computational approaches in genomics, proteomics and transcriptomics*. Boston, MA: Springer Science+Business Media, LLC.
Yamada, E. A., & Sgarbieri, V. C. (2005). Yeast (saccharomyces cerevisiae) protein concentrate: preparation, chemical composition, and nutritional and functional properties. *Journal of Agricultural and Food Chemistry*, *53*(10), 3931–3936.